The Structure and Dynamics of the Ocean Surface Mixed Layer

G. L. MELLOR AND P. A. DURBIN

Geophysical Fluid Dynamics Program,[1] Princeton University, Princeton, N. J. 08540

(Manuscript received 15 January 1975, in revised form 2 June 1975)

ABSTRACT

The present paper describes a one-dimensional unsteady model of the ocean surface mixed layer. The model somewhat resembles the approach of Munk and Anderson in that the differential equations for mean velocity and temperature are solved. The Richardson-number-dependent stability functions which enter the model are significantly different, however, as is the fact that we are able to solve problems with realistic boundary conditions. Furthermore, all empirical constants have been determined from neutral turbulent flow experiments.

Comparisons of prediction and data are favorable.

1. Introduction

The present paper follows the approach of Ekman (1905) and Munk and Anderson (1948) in that the Reynolds differential equations for turbulent ocean layers is the starting point; mixing coefficients for momentum and heat must then be provided empirically. While Munk and Anderson did specify Richardson-number-dependent mixing coefficient functions, a peculiarity of these functions rendered it impossible to satisfy boundary conditions for velocity. Now, however, considerably more *a priori* information is available concerning the effect of the Richardson number and, in fact, there exists more experience on ways of modeling turbulent momentum and heat flux in the neutral case. The object here is to combine these elements and determine their efficacy in predicting observed features of the mixed layer and thermocline. In the present model all empirical constants are obtained from neutral turbulence data. Numerical calculations are restricted to horizontally homogeneous layers but stationary and nonstationary (hereafter referred to as steady and unsteady) flows may be treated.

A Richardson-number-dependent stability function is derived from the turbulent equations in other papers (Mellor, 1973; Mellor and Yamada, 1974; henceforth to be referred to as papers I and II) for the case where unsteady and diffusive terms are neglected in favor of a balance between kinetic and potential turbulent energy production terms and dissipation. A critical gradient Richardson number, beyond which turbulence virtually cannot exist, of 0.23 is derived, a result which is supported by the atmospheric surface layer data of Businger *et al.* (1971) and the analysis of paper I, by an analogous and corroborative study of boundary layer curvature effects (So and Mellor, 1973; Mellor 1975), and, we believe, by the present results although the data we use here are less detailed and less directly supportive of this statement.

In view of stability analyses [see Chapter 4 of Turner (1973) for a summary], it appears that a local Richardson number in the range 0.21–0.25 is emerging as a remarkably general criterion for the existence of turbulence.

Most of the recent mixed layer theories (Turner and Kraus, 1967; Kraus and Turner, 1967; Kitaigorodsky and Miropolsky, 1970; Denman, 1973; Denman and Miyake, 1973; Pollard *et al.*, 1973; Niiler, 1975) have been integral theories. The advantage of integral methods is their apparent simplicity whereby distributed quantities are lumped into integral values. Special solutions often emerge in closed analytical form. On the other hand, these theories involve fairly complicated assumptions concerning the vertical profiles of velocity, temperature, heat flux and stress, and for example, integral theories do not predict the existence of a mixed layer and thermocline as a consequence of oceanic boundary conditions; existence must be assumed, *a priori*. Thus, integral mixed layer and upper thermocline theories are disconnected from available information on other turbulent boundary layer flows including neutral flows; they are tailored to a restricted subset of possible boundary conditions. Nevertheless, integral representations of mixed layer dynamics may be a computational requirement for numerical, oceanic general circulation models. If credence in the present approach is developed, then the calculated results, wherein many mean and turbulent properties are specifically identified, may be useful in assessing existing integral models or in suggesting modifications.

[1] Support provided through Geophysical Fluid Dynamics Laboratory/NOAA Grant 04-3-022-33.

2. The model

The equations we plan to solve for a variety of boundary conditions are

$$\frac{\partial U}{\partial t}-fV=\frac{\partial}{\partial z}\left(-\overline{wu}+\nu\frac{\partial U}{\partial z}\right), \tag{1a}$$

$$\frac{\partial V}{\partial t}+fU=\frac{\partial}{\partial z}\left(-\overline{wv}+\nu\frac{\partial V}{\partial z}\right), \tag{1b}$$

$$\frac{\partial \Theta}{\partial t}+W\frac{\partial \Theta}{\partial z}=\frac{\partial}{\partial z}\left(-\overline{w\theta}+\nu_T\frac{\partial \Theta}{\partial z}\right), \tag{2}$$

where z, t are the vertical (positive upward) space coordinate and time, f the Coriolis parameter, U, V the mean velocity components relative to the geostrophic velocity, Θ the mean temperature, and $-\overline{wu}$, $-\overline{wv}$ and $-\overline{w\theta}$ the turbulent Reynolds stress and heat flux (divided by density and the product of density and specific heat, respectively). The basic assumption involved in neglecting the advective momentum terms in (1a, b) is that the Rossby number based on a characteristic velocity and horizontal length scale is small. In (2), horizontal advection has been neglected. For the transient short-time scale problems discussed below where the tendency term is much larger than horizontal advection, this is not a serious restriction. In the present paper we have included vertical advection merely as a convenience to generate an initial temperature profile resembling a thermocline profile. The molecular kinematic viscosity and thermal diffusivity are included in (1a, b) and (2). As discussed below, our results are not sensitive to the values of ν and ν_T so long as they are not zero.

According to the "Level 2" model of paper II we define

$$(-\overline{uw},\ -\overline{vw})=lq\tilde{S}_M\left(\frac{\partial U}{\partial z},\ \frac{\partial V}{\partial z}\right), \tag{3a, b}$$

$$-\overline{\theta w}=lq\tilde{S}_H\frac{\partial \Theta}{\partial z}, \tag{4}$$

which is a traditional K theory format. However $q^2\equiv\overline{u^2}+\overline{v^2}+\overline{w^2}$ is twice the turbulent kinetic energy, and $\tilde{S}_M$ and $\tilde{S}_H$ are flux-Richardson-number-dependent stability factors, *derived* in paper II, wherein three empirical constants are required but are determined once and for all from neutral turbulent flow data.[2] The functions are plotted in Fig. 1. If we define β as the coefficient of thermal expansion and g the gravity constant, the flux Richardson number is defined according to

$$R_f\equiv\frac{-\beta g\overline{w\theta}}{-\overline{wu}\dfrac{\partial U}{\partial z}-\overline{wv}\dfrac{\partial V}{\partial z}}, \tag{5}$$

i.e., the ratio of the (negative) turbulent energy production due to buoyancy to the production due to shear. When $R_f>0.21$, $\tilde{S}_M=\tilde{S}_H=0$. In this model q is determined from the turbulent energy equation

$$-\overline{wu}\frac{\partial U}{\partial z}-\overline{wv}\frac{\partial V}{\partial z}+\beta g\overline{w\theta}-\frac{q^3}{B_1 l}=0, \tag{6}$$

representing a balance between shear production, buoyancy production and dissipation. The dissipation, $\overline{\nu(\partial u_i/\partial x_k)^2}$, is modeled according to the last term in (6) where $B_1=15.0$ is one of the aforementioned constants. Thus, this model neglects diffusion and advection of turbulent energy, quantities which may be included by recourse to the Level 3 or 4 models of paper II. However, these terms are relatively small in the present context as has been determined diagnostically. That is, they are small relative to the dominant energy transfer through the mean kinetic and potential ener-

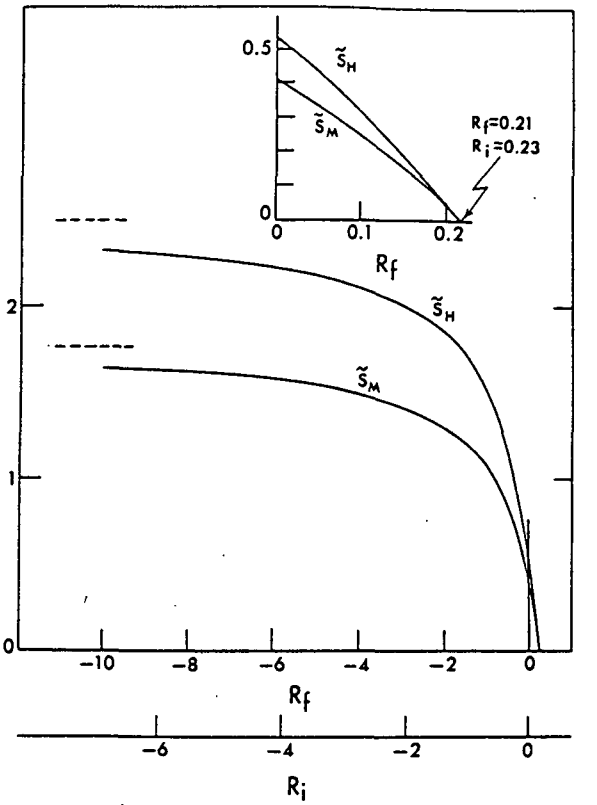

FIG. 1. The functions $\tilde{S}_M$ and $\tilde{S}_H$. Inset is a detail for $R_f>0$.

[2] $\tilde{S}_H=3A(\gamma_1-\gamma_2\Gamma)$ and $\tilde{S}_M=\tilde{S}_H[3A(\gamma_1-C-9A\Gamma/B_1)]/[\gamma_1-\gamma_2\Gamma+3A\Gamma/B_1]$, where $\Gamma\equiv R_f/(1-R_f)$, $\gamma_1\equiv(\frac{1}{3})-(2A/B_1)$, $\gamma_2\equiv(B_2/B_1)+(6A/B_1)$ and $(A, B_1, B_2, C)=(0.78, 15.0, 8.0, 0.056)$. These constants are constrained according to $B_1=[A(B_1-6A-3B_1C)]^{\frac{1}{3}}$ so that only three may be chosen independently. The critical condition, $\tilde{S}_M=\tilde{S}_H=0$, is given by $\Gamma_C=\gamma_1/\gamma_2$ or $R_{fC}=0.21$.

gies. Equations for the latter can be obtained from (1a, b) and (2); thus, after multiplying (1a, b) and (2) by U, V and $-\beta gz$ we obtain the diagnostic equations:

$$\frac{\partial}{\partial t}\left(\frac{U^2+V^2}{2}\right)+\frac{\partial}{\partial z}\left(U\overline{wu}+V\overline{wv}-\nu\frac{\partial U^2/2}{\partial z}\right)=\overline{wu}\frac{\partial U}{\partial z}+\overline{wv}\frac{\partial V}{\partial z}-\nu\left(\frac{\partial U}{\partial z}\right)^2, \quad (7)$$

$$\frac{\partial}{\partial t}(-\beta gz\Theta)+\frac{\partial}{\partial z}\left(-\beta gz\overline{w\theta}+\beta g\nu_T\frac{\partial \Theta}{\partial z}\right)=-\beta g\overline{w\theta}+\beta g\nu_T\frac{\partial \Theta}{\partial z}. \quad (8)$$

The first terms on the right of (7) and (8) represent the flow of mean energy into turbulent kinetic energy which, according to (6), is dissipated locally and with no lag. The spatial transfer of mean energy is accomplished through the second terms on the left side of (7) and (8).

To complete the model it is necessary to specify the length scale which enters (3a, b), (4) and (6). As discussed in paper II and in the paper by Mellor and Herring (1973), we have considered some of the more complicated proposals for length scales and, for a variety of reasons, are somewhat skeptical of their physical viability. The simplest prescription would seem to be the ratio of the first to the zeroth moment of the turbulence field as defined by

$$l=\alpha\frac{\int_{-\infty}^{0}|z|q dz}{\int_{-\infty}^{0}q dz}, \quad (9)$$

where α is another constant; in paper II we decided that $\alpha=0.10$ would yield a neutral Ekman layer (in conformance with our methodology that all constants be determined from neutral turbulence flow data) such that it's outer edge is somewhat larger than $0.3u_\tau/f$ where $u_\tau\equiv|\tau|_{z=0}^{\frac{1}{2}}$; this value is somewhat uncertain since a "pure" Ekman layer is hard to find in nature (Gill, 1969; Deardorff, 1970, 1973; Caldwell *et al.*, 1972).

However, our results appear to be surprisingly insensitive to a choice of α. For example, for the impulsive wind calculations described below, the values $\alpha=0.05$ and 0.10 gave virtually identical temperature profiles whereas U, V and q^2 were—on the surface—roughly 20% higher when $\alpha=0.05$.

In paper II, in applying the model to atmospheric boundary layers, we had matched the constant value of l given in (9) to $l\sim\kappa z$ as $z\to 0$ where κ is the von Kármán constant. This, of course, yields a near-surface logarithmic velocity behavior. In the present application, this strategy is also possible. The principal effect would be larger mean velocities near the surface while not affecting other results significantly. In view of the uncertainties of sea surface-wave interactions, the present simplification seemed reasonable, however.

For the surface boundary conditions one may either stipulate the sea surface temperature

$$\Theta(0,t)=\Theta_s(t), \quad (10a)$$

or the surface heat flux

$$\left[(ql\tilde{S}_H+\nu_T)\frac{\partial \Theta}{\partial z}\right]_{z=0}=H(t), \quad (10b)$$

and a surface wind stress

$$\left[(ql\tilde{S}_M+\nu)\frac{\partial U}{\partial z}\right]_{z=0}=\tau_{0x}(t), \quad \left[(ql\tilde{S}_M+\nu)\frac{\partial V}{\partial z}\right]_{z=0}=\tau_{0y}(t). \quad (11)$$

At some depth, $z=-D$, we let

$$\Theta(-D,t)=\Theta_D, \quad (12)$$

$$U(-D,t)=V(-D,t)=0. \quad (13)$$

Method of Solution

To solve the equations we have chosen a two-time-step, implicit algorithm[3] wherein the z integration proceeds via the standard tri-diagonal matrix reduction technique (Richtmyer and Morton, 1967). At each time step, an iteration was performed to determine the coefficients, $lq\tilde{S}_M$ and $lq\tilde{S}_H$, using (5), (6), (9) and the functions, $\tilde{S}_H(R_f)$ and $\tilde{S}_M(R_f)$. In actual fact, while the above equations are complete, we found that convergence is improved if, instead of (5), we evaluate the gradient Richardson number

$$\mathrm{Ri}\equiv\frac{\beta g\dfrac{\partial \Theta}{\partial z}}{\left[\left(\dfrac{\partial U}{\partial z}\right)^2+\left(\dfrac{\partial V}{\partial z}\right)^2\right]} \quad (14)$$

in the course of iteration after which

$$R_f=0.725[\mathrm{Ri}+0.186-(\mathrm{Ri}^2-0.316\,\mathrm{Ri}+0.0346)^{\frac{1}{2}}]. \quad (15)$$

The latter relation can be obtained from (3a, b), (4),

[3] Thus, if $h\equiv u+iv$, we have in place of (1a, b) and (3a, b)

$$\partial h/\partial t+ifh=\partial[(\nu+lq\tilde{S}_M)\partial h/\partial z]/\partial z\equiv D.$$

The time differencing is $h^{n+1}-h^n+if\Delta t(h^{n+1}+h^n)/2=\Delta tD^{n+1}$. Stresses, heat flux and turbulent energy were evaluated midway between the vertical grid points where mean velocity and temperature were determined. See Kurihara (1965) for further discussion of this differencing scheme.

(5), (6), the functions $\tilde{S}_H(R_f), \tilde{S}_M(R_f)$ and the necessary empirical constants. When $R_f=0$ and 0.21, Ri=0 and 0.23, respectively.

3. Response to an impulsive wind stress

The first problem we will examine with our model is that of a quiescent ocean subject to an impulsively applied surface wind stress. In particular

$$\tau_{0y}=0, \quad \tau_{0x}=\begin{cases}0, & t\leqslant 0\\ 2\ \text{cm}^2\ \text{s}^{-2}, & t>0.\end{cases}$$

The initial temperature was calculated for zero stress by applying a surface heat flux and choosing values of W and ν_T. However, for $t>0$ the surface heat flux and W were set equal to zero; the choice of ν_T for $t>0$ will be discussed below. The particular initial profile was selected to approximate station "Papa" data below the mixed layer. This data will be examined later. Also we have set $\beta g=-1.73\times10^{-3}$ m s^{-2} K^{-1} and $f=10^{-4}$ s^{-1}. The vertical grid resolution was 1 m.

Fig. 2 depicts the variation of temperature for $0\leqslant t/T\leqslant 4$, where $T=2\pi f^{-1}$ is the inertial period. The integrating increment is $\Delta t/T=0.05$. In Fig. 3 we show the development of the velocity at different depths and the Ekman transport which was obtained diagnostically by vertically integrating the velocity profiles. Since the Ekman transport for this problem is

$$(S_x,S_y)\equiv\left(\int_{-D}^{0}U\,dz,\int_{-D}^{0}V\,dz\right)$$
$$=(\tau_{0x}/f)(\sin2\pi t/T,\ -1+\cos2\pi t/T),$$

one has a diagnostic check on the numerical algorithm.

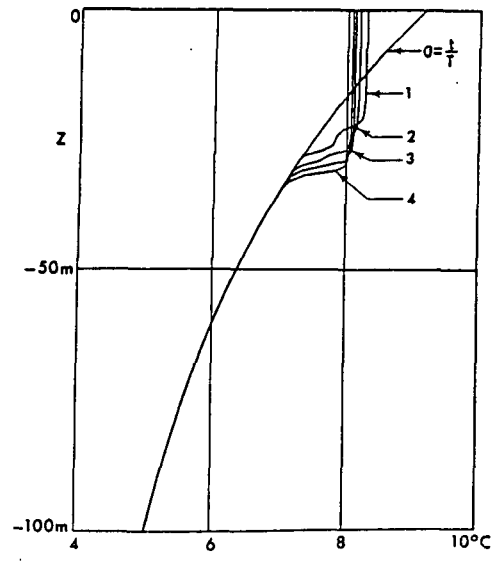

FIG. 2. Variation of temperature due to an impulsive wind: $\tau_{0x}=2$ cm^2 s^{-2} when $t>0$.

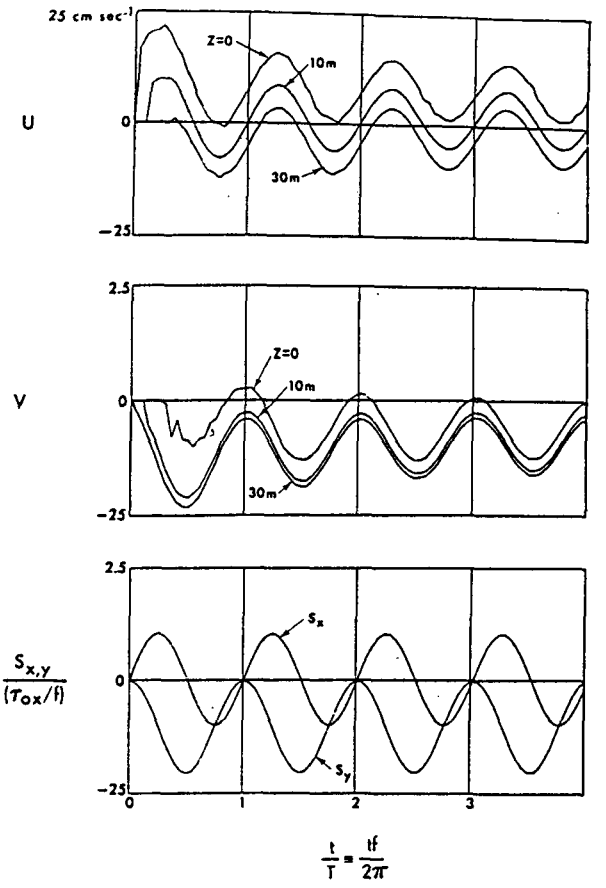

FIG. 3. Response of the velocity field and the vertically integrated Ekman transport, $\tilde{S}_x$, $\tilde{S}_y$.

In Fig. 4, the vertically integrated energy budget has been plotted. For $W=0$ Eqs. (7) and (8) may be written

$$\frac{d\text{KE}}{dt}+\text{Work}+\text{SP}=0, \tag{16a}$$

$$\frac{d\text{PE}}{dt}+\text{BP}=0, \tag{16b}$$

where

$$\text{KE}\equiv\int_{-D}^{0}\frac{U^2+V^2}{2}dz \tag{17a}$$

$$\text{Work}\equiv(U\overline{wu}+V\overline{wv})_{z=0} \tag{17b}$$

$$\text{SP}\equiv\int_{-D}^{0}\left(-\overline{wu}\frac{\partial U}{\partial z}-\overline{wv}\frac{\partial V}{\partial z}\right)dz \tag{17c}$$

$$\text{PE}\equiv\int_{-D}^{0}(-\beta gz\Theta)dz \tag{17d}$$

$$\text{BP}\equiv\int_{-D}^{0}g\beta\overline{w\theta}dz. \tag{17e}$$

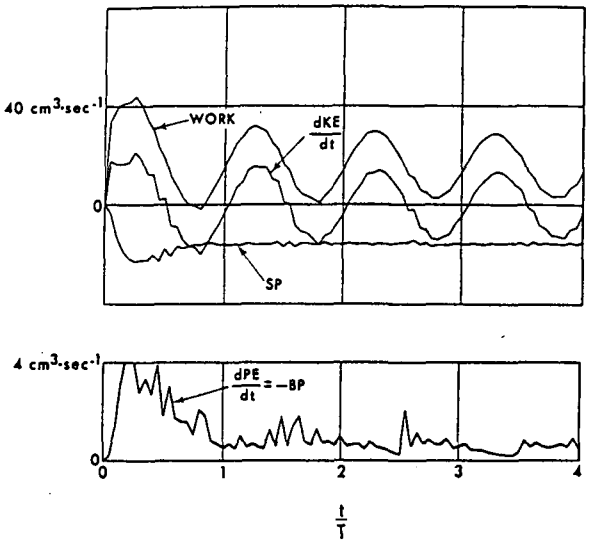

FIG. 4. Vertically integrated energy budget.

Here the shear production SP and buoyancy production BP produce turbulence which according to (6) is immediately dissipated.

It will be noted that we have neglected the viscous terms in (16a, b); they are indeed negligible. In Fig. 4 it will also be noted that BP is more than an order of magnitude smaller than SP and makes a negligible contribution to the *integrated* turbulent energy budget. However, $\beta g\overline{w\theta}$ is *locally* important at the interface of the mixed layer and the deeper stable thermocline. To see this we need the logarithmic plot of Fig. 5. At sufficiently large depth, $-\overline{uw}\partial U/\partial z - \overline{vw}\partial V/\partial z$ has decreased and $-\beta g\overline{w\theta}$ increased so that $R_f \approx 0.21$; below this, all turbulent energy production is zero since $\bar{S}_M = \bar{S}_H = 0$.

It will be noted that the wind stress work oscillates in direct relation to $U(0,t)$ and, somewhat surprisingly,

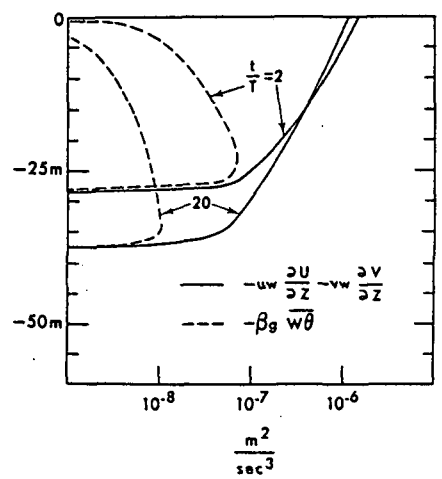

FIG. 5. Vertical distribution of turbulent production by shear and buoyancy.

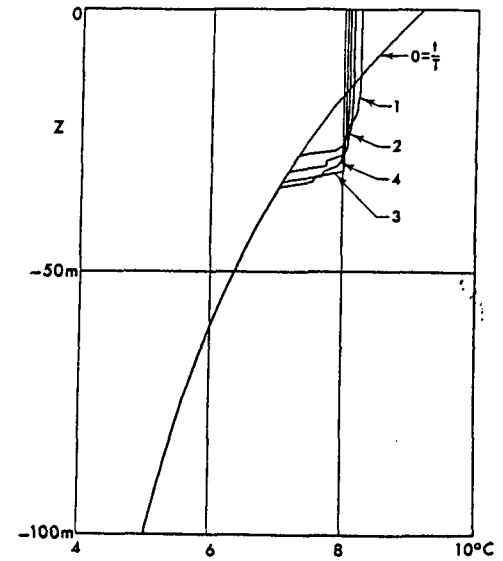

FIG. 6. Calculation similar to Fig. 2, except that the values of molecular diffusivity were used for ν and ν_T.

the rate of storage of kinetic energy, $d\mathrm{KE}/dt$, compensates the oscillatory component of the work such that SP, after the initial transient, is almost exactly constant in time.

Now, it is *almost* possible to state that, whereas viscosity is ultimately responsible for dissipation [the right-hand term in (6) is our viscosity-independent model for viscous dissipation[4]], our results are independent of viscosity. As is easy to imagine, viscosity must be important at the interface. However, we have inserted molecular values ($\nu = 0.0134$ cm² s^{-1}, $\mathrm{Pr} \equiv \nu/\nu_T = 10$) and have also increased these values by factors of 10; the detailed effect is that low values of viscosity give rise to a "jittery" calculation (the effect is magnified in BP of Fig. 4) whereas larger viscosities smooth out this effect; all of this relates to the fact that we do not adequately resolve the detailed structure of the mixed layer interface. This, of course, has been a matter of some concern. Nevertheless, all runs with various ν and ν_T yield essentially the same average results. The results discussed above were for $\nu = \nu_T = 0.134$ cm² s^{-1}. In Fig. 6 are temperature profiles for the molecular values, $\nu = 10\nu_T = 0.0134$ cm² s^{-1}. All of these numbers can be contrasted with the values $lq\bar{S}_M \approx 100$–300 cm² s^{-1} calculated throughout most of the mixed layer.

In all of the above discussion, we make no judgment as to physically realistic values of ν or ν_T. Our model predicts zero turbulent mixing below the mixed layer and does not (presently) account for other processes such as nonlinear internal wave effects which could yield effective values larger than molecular. For ex-

[4] It is well known that viscosity does not control the dissipation rate but merely sets the smallest scales at which dissipation predominantly occurs.

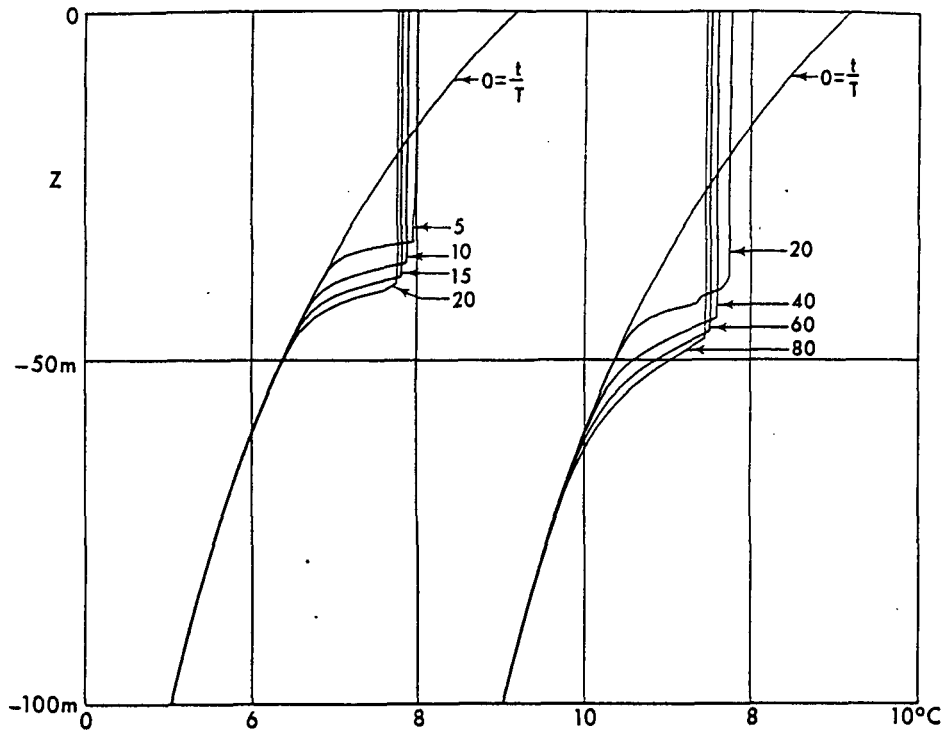

FIG. 7. Calculations using larger time steps: left side, $\Delta t/T=\frac{1}{4}$; right side, $\Delta t/T=1$.

ample, Veronis (1969) estimates the values

$$\nu \approx \nu_T \approx 0.2 \text{ cm}^2 \text{ s}^{-1}.$$

A further point to make is that the aforementioned calculation "jitteriness" would probably not be present in a Level 3 model since diffusive and tendency terms introduced into the turbulent energy equation (6) would smooth out variables near the mixed layer interface although it will still remain relatively sharp (see paper II). We will probably adopt the Level 3 model for future work, partially to realize this advantage. However, for this paper, the advantage of the more simple turbulent energetics in promoting conceptual understanding of an already complicated problem was thought to be compelling; the loss in predictive accuracy is probably not significant.

To run the model for longer periods of time we have simply increased the time increment, $\Delta t/T$, to 0.25 and 1.0 (from the former calculation a shear and buoyancy production profile has already been included in Fig. 5). The temperature profiles in Fig. 7 show practically no truncation error; that is, the $\Delta t/T=0.25$ calculations agree with the previous $\Delta t/T=0.05$ where they overlap and the $\Delta t/T=1.0$ calculation agree with $\Delta t/T=0.25$ where they overlap. As shown in Fig. 8 the median time step resolves the inertial oscillations to a certain extent, although a phase error is readily apparent, whereas no inertial information is retained in the largest time step calculation. However, the average energy budgets of the three calculations agree in the overlapping time intervals. Therefore, where a knowledge of the unsteady component of the velocity is not necessary, it would appear that quite large time steps are possible.

In Fig. 9, the time evaluation of the mixed layer depth $h(t)$ is plotted semi-logarithmically; h is chosen

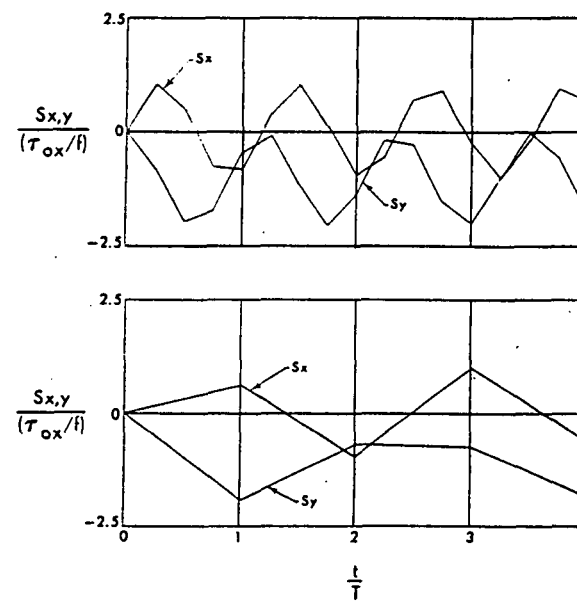

FIG. 8. Ekman transport for larger time steps: top, $\Delta t/T=\frac{1}{4}$; bottom, $\Delta t/T=1$.

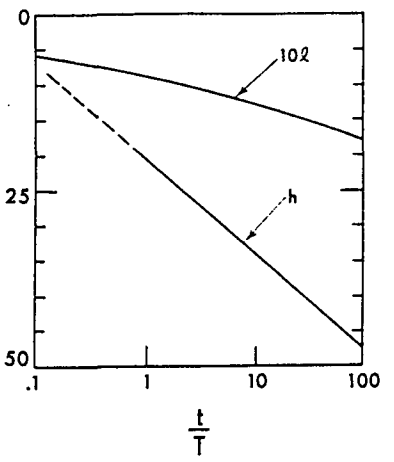

FIG. 9. Semi-logarithmic plot of h and $10\,l$ versus t/T.

at the point where the temperature began to depart significantly from a constant. For $t/T<1$, this was difficult to judge within 10–15% so we entered in a dashed line. Although a decrease in the rate of penetration is expected with time (from Fig. 9, we obtain $dh/dt=-5.86\ m/t$), we have no simple physical reason for a logarithmic behavior, *per se*.

It will be noted that the foregoing equations and results could be non-dimensionalized using the length, velocity, temperature and time scales given by u_τ/f, u_τ, β and $T=2\pi/f$, where $u_\tau^2\equiv\tau_{0x}$. If we characterize the initial temperature gradient by a constant value, $(\partial\Theta/\partial z)_0$, then a family of solutions could be calculated which are parametric in N_0^2/f^2 where N_0 is the initial Brunt-Väisälä frequency $(\beta g\partial\Theta/\partial z)_0^{\frac{1}{2}}$. In the present case (based on the surface temperature gradient) $N_0^2/f^2=1.31$.

4. After the wind stops

After the wind stops the calculations indicate no further deepening of the mixed layer. If the wind stops when $S_x=S_y=0$ it may easily be shown that $S_x=S_y=0$ thereafter. Furthermore the velocity and turbulence fields decay very quickly. Otherwise, the mean velocity field persists as is shown in Fig. 10 where a "slab" flow field develops wherein the velocity as well as the temperature is very nearly constant in the mixed layer. According to our calculations most of the decay of mean velocity *gradients* takes place in a short time interval, less then about $0.2T$, after which the turbulence is also negligible. Evidently, the remaining kinetic energy is thereafter removed by viscosity on a time scale very much longer than treated here.

5. Application of a sudden surface heat flux

We now maintain the wind stress constant at 2 cm^2 s^{-2} and, as initial velocity and temperature conditions, use the calculated fields at $t/T=5$; then a surface heat flux is suddenly imposed. Somewhat arbitrarily we chose a rather large value, $H=\pm10^{-2}$ cm K s^{-1}; the plus value is heating while the negative value is cooling. The results are seen in Fig. 11. In Fig. 12 we have repeated the calculation using a lower wind stress of 1 cm^2 s^{-2}.

6. Station Papa data

In Fig. 13 we compare the observed station Papa data (Denman and Miyake, 1973; Minkley, 1971), collected at 50°N, 145°W, and the calculated isotherms on a time-depth plot.

The measured surface temperature was an input to the calculation as well as the measured variable wind velocity magnitude and direction. (The average winds were southwesterly.) A drag coefficient $C_{10}=0.002$ was used.

Aside from the fact that small-scale variations are not predicted—since there is no vertical velocity varia-

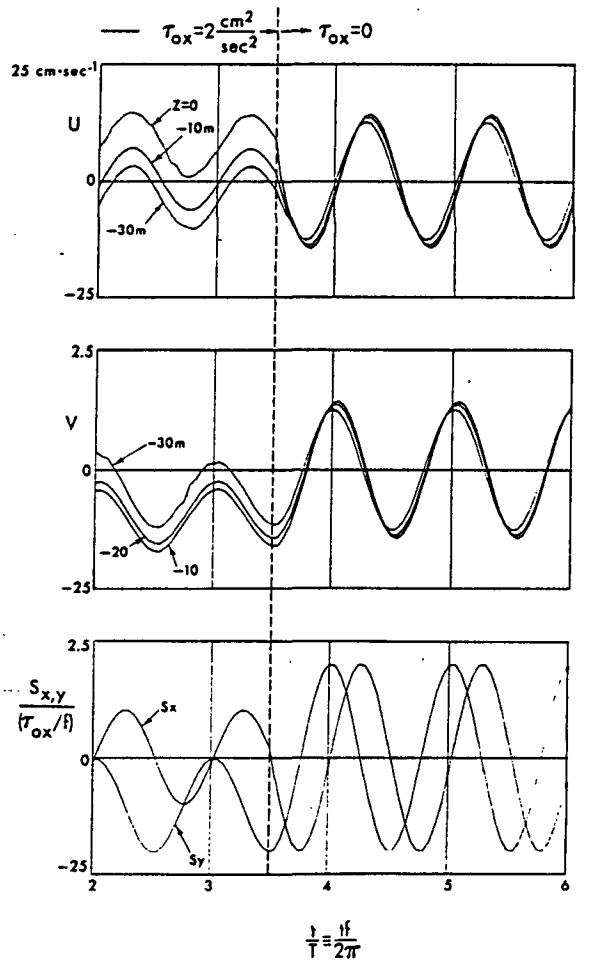

FIG. 10. Effect of the wind stopping at $t/T=3.5$ when $(S_x^2+S_y^2)^{\frac{1}{2}}$ is maximum. When the wind stops at $t/T=4.0$ the entire velocity field decays rapidly.

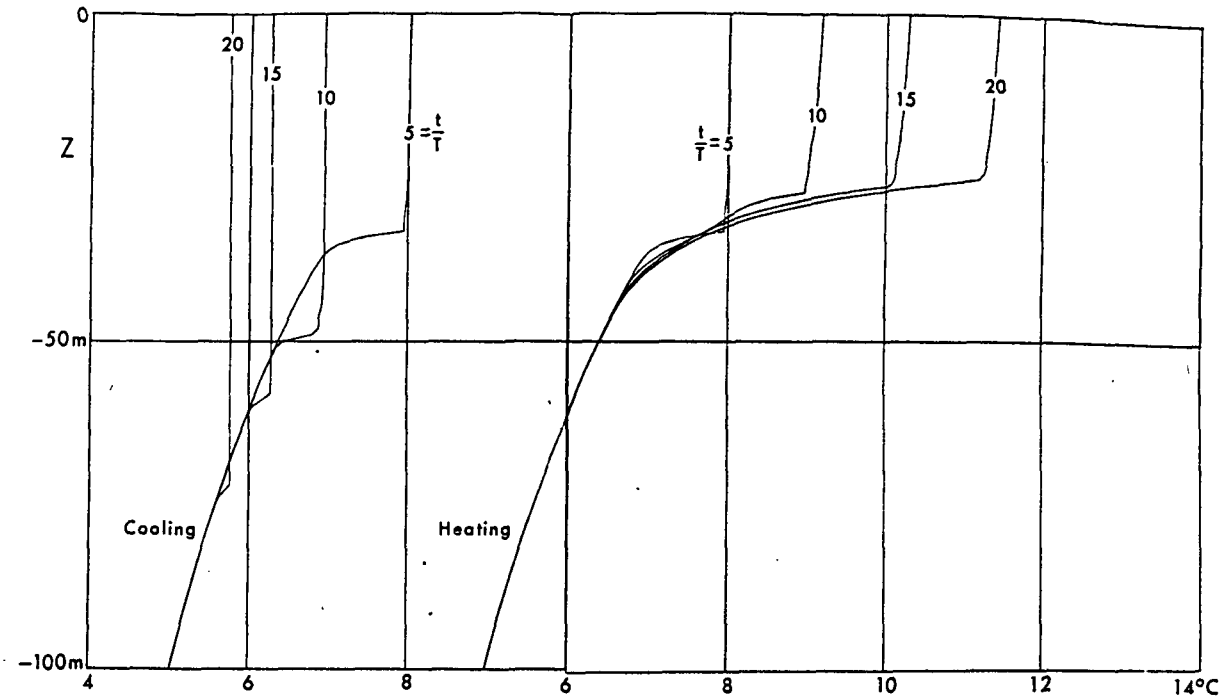

FIG. 11. Effect of sudden heating or cooling: $\tau_{0x} = 2$ cm^2 s^{-2}.

tion in our model—the mixed layer penetration is predicted fairly well. Note that we have not yet included radiation penetration in the model. Another point to make is that, in the data under consideration, the salinity is quite uniform in the upper 100 m. Nevertheless, we take $\rho - \rho_0 = \rho_0 \beta(\theta - \theta_0)$ where β as used in (5) has been adjusted to account for salinity variations (Fofonoff, 1962) which are assumed to be proportional to temperature.

It should be stressed again that no constants were

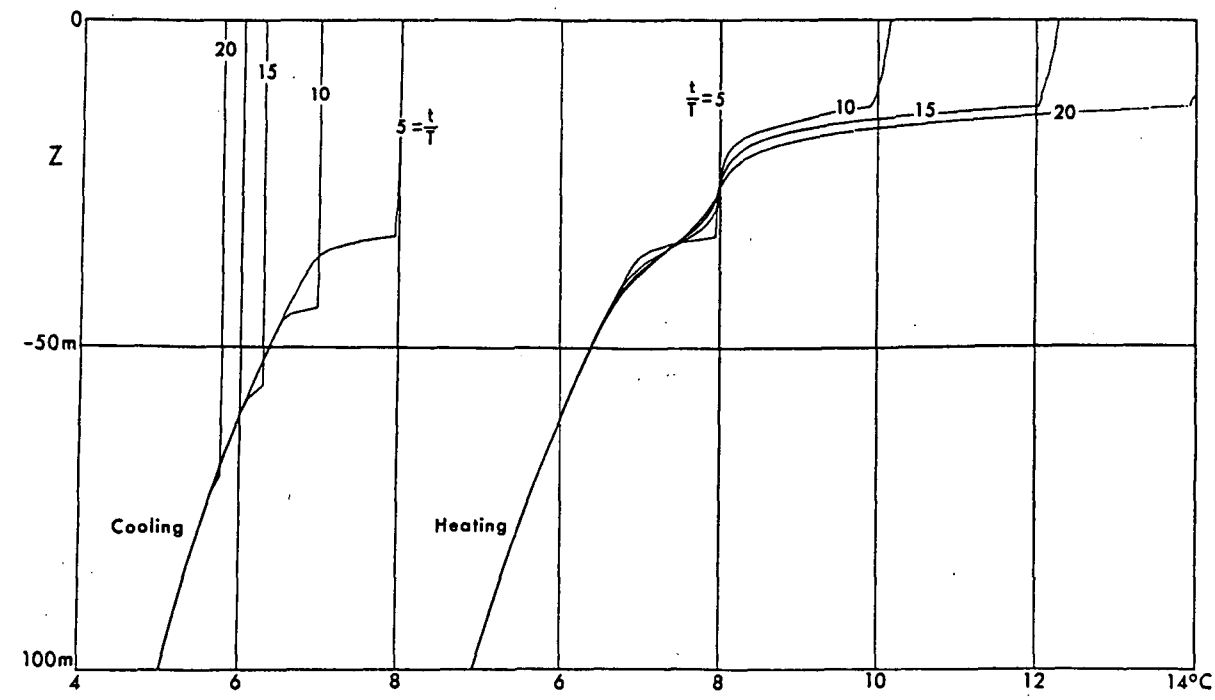

FIG. 12. Effect of sudden heating or cooling: $\tau_{0x} = 1$ cm^2 s^{-1}.

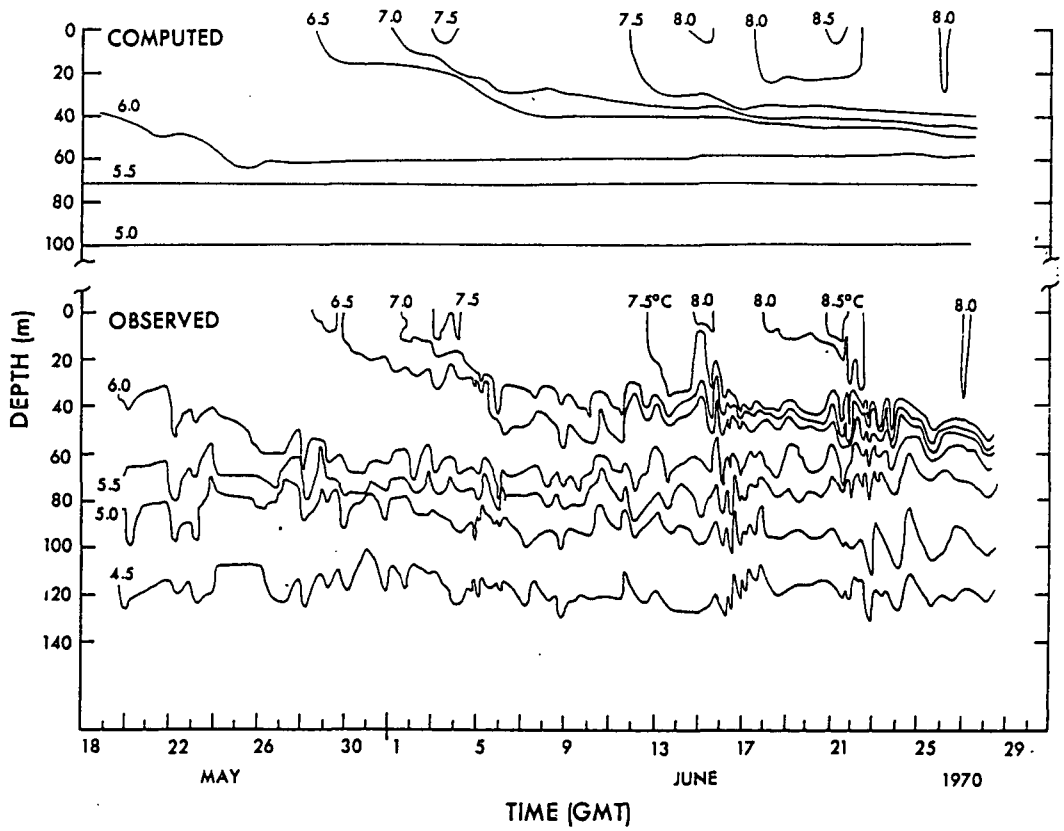

FIG. 13. Comparison of computed and observed time-depth isothermal contours at station Papa. The boundary conditions were the observed surface temperature and wind stress.

adjusted to improve agreement between data and calculations.

7. Stratified turbulent Raleigh flow

Kato and Phillips (1969; hereafter K & P) have provided a rather nice set of data from an experiment which approximately corresponds to the sudden acceleration of a horizontal screen near the surface of salt-stratified fluid in a channel of rectangular cross section. After a short initial time the imposed surface shear stress was nearly constant. Mixed layer penetration was observed with the help of dye. The channel was actually an annulus; hopefully, the effects of curvature were unimportant.

Our first prediction of mixed layer penetration of one of the K & P cases was remarkably good. (Fig. 14 is a result of the calculation, presented here since it might be helpful in visualizing the problem.) The prediction of a second case was high by 20–25%.

We then noted that if one prediction was good, all predictions should be, since the governing equations (and, presumably, the experimental data) can be cast in a similar, parameter-free form. Thus, if the initial Brunt-Väisälä frequency is $N\equiv[g(\partial\rho/\partial z)_{t=0}/\rho_0]^{\frac{1}{2}}$ and if we let

$$z=u_\tau\tilde{z}/N,\quad t=\tilde{t}/N,\quad U=u_\tau\tilde{U},\qquad (18a, b, c)$$

$$\rho=\rho_0(1+u_\tau N\tilde{\rho}/g),\quad q=u_\tau\tilde{q},\qquad (18d, e)$$

the appropriate equations are

$$\frac{\partial\tilde{u}}{\partial\tilde{t}}=\frac{\partial}{\partial\tilde{z}}\left[(\tilde{l}\tilde{q}\tilde{S}_M+\tilde{\nu})\frac{\partial\tilde{U}}{\partial\tilde{z}}\right],\qquad (19a)$$

$$\frac{\partial\tilde{\rho}}{\partial\tilde{t}}=\frac{\partial}{\partial\tilde{z}}\left[(\tilde{l}\tilde{q}\tilde{S}_H+\tilde{\nu}_S)\frac{\partial\tilde{\rho}}{\partial\tilde{z}}\right],\qquad (19b)$$

where also $(\nu,\nu_s)=(N/u_\tau^2)(\tilde{\nu},\tilde{\nu}_s)$. Eq. (6) can be also non-dimensionalized whence $-\beta\overline{w\theta}$ is replaced by $\overline{w\rho}'$ and the Richardson number is $\mathrm{Ri}\equiv(\partial\tilde{\rho}/\partial\tilde{z})/(\partial\tilde{u}/\partial\tilde{z})^2$. The boundary conditions are

$$\tilde{u}\sim 0,\ \tilde{\rho}\sim-\tilde{z},\quad \text{as } \tilde{z}\to-\infty.\qquad (20a, b)$$

Note that $\tilde{\nu}$ is of the order 10^{-2} and $\tilde{\nu}_s$ based on the diffusivity of salt is much smaller. The measurements and our calculations agree that the overall results are independent of Reynolds number. Thus, $\tilde{u}$, $\tilde{\rho}$ are universal functions of $\tilde{z}$ and $\tilde{t}$.

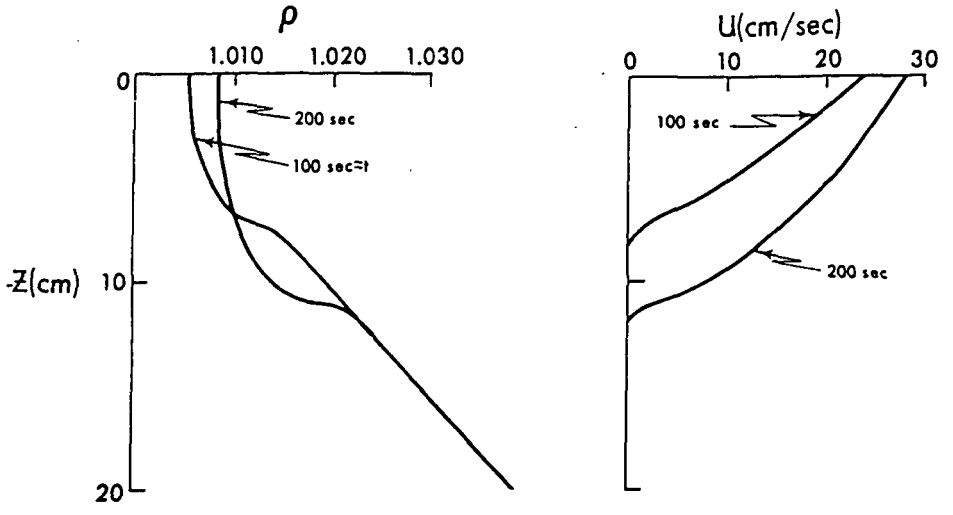

FIG. 14. Computed profiles corresponding to the Kato and Phillips experiment where $(d\rho/dz)_0/\rho_0 = 1.92\times10^{-3}$ cm^{-1} and $\tau_0 = 0.995$ cm^2 s^{-2}.

Now rather than look at each individual case, it is possible to directly compare our calculated results with the summary plot of entrainment rate, provided by K & P. We first define an entrainment function

$$E \equiv \frac{dh/dt}{u_\tau}, \tag{21a}$$

and a bulk Richardson number

$$Ri_0 \equiv \frac{N^2h^2}{2u_\tau^2}. \tag{21b}$$

In Fig. 15 the calculated result is shown in comparison with the data. Note that K & P consider departure from the form $E = E(Ri_0)$ to be experimental scatter; we agree, since at the very least we believe our model is properly scaled.

Pollard *et al.* (1973) have proposed a simple model with assumed step profiles for mixed layer velocity and density. A bulk Richardson number based on the penetration depth and the step density and velocity increment was assumed to be unity. According to their model the neat result that

$$h = 2^{\frac{1}{2}}u_\tau(t/N)^{\frac{1}{2}} \tag{22a}$$

or

$$E = \frac{Ri_0^{-\frac{1}{2}}}{2} \tag{22b}$$

can be obtained and is drawn in Fig. 15.

In our own computer runs it is possible to approximately calculate another bulk Richardson number, defined as

$$B \equiv \frac{gh\Delta\rho/\rho_0}{(\Delta u)^2},$$

according to Pollard *et al.*, where $\Delta\rho$ is the density jump across the interface based on an average mixed layer

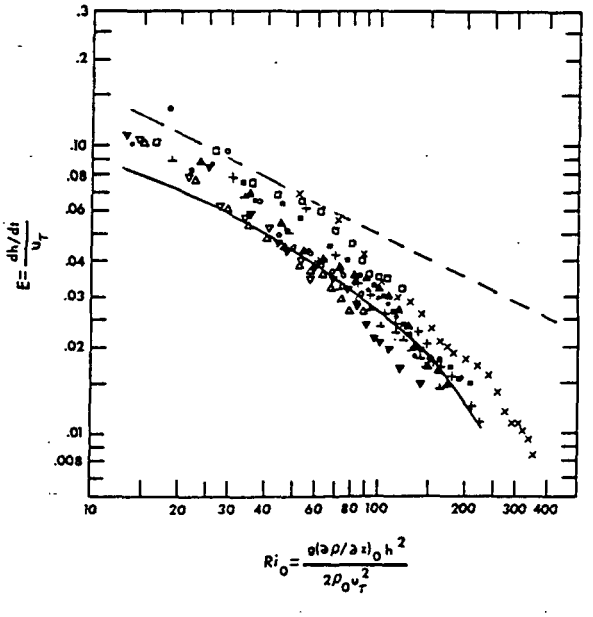

FIG. 15. The entrainment function $E = (dh/dt)/u_\tau$ as a function of a bulk Richardson number. The detailed legend for the data is given in Kato and Phillips (1969). [Solid, open and crossed-line symbols correspond to $(d\rho/dz)/\rho_0 = 1.92$, 3.84, 7.96×10^{-3} cm^{-1}, respectively, whereas τ_0 ranged from 0.995–2.75 cm^2 s^{-2}.] The solid line is computed here whereas the dashed line is predicted by the theory of Pollard *et al.* (1973).

density and Δu the average mixed layer velocity. If we repeat their analysis, we obtain[5]

$$E=\frac{B^{\frac{1}{2}}}{2}Ri_0^{-\frac{1}{2}} \tag{23}$$

instead of (22b). Our numerical results (e.g., see Fig. 8), when the calculated profiles are approximated by step profiles, yield $B\approx 0.35$. Without drawing another line in Fig. 15, it will be seen that this value used in (23) represents some improvement over (22b).

8. Summary

The rather simple model discussed here is not unlike that proposed by Munk and Anderson (1948). However, we have been able to incorporate realistic boundary conditions and these together with Eqs. (3a, b), (4) and (6) have produced rather realistic and detailed results for a wide variety of boundary conditions. The model itself is quite simply stated being comprised of Eqs. (3a, b), (4), (5), (6), and the functions $\tilde{S}_M(\mathrm{Ri})$ and $\tilde{S}_H(\mathrm{Ri})$. The momentum and energy equations have been simplified to (1a, b) and (2) in the present study but, of course, advective terms can be reinstated if one is prepared to cope with the requisite numerical effort.

It should be noted that no empirical numbers have been adjusted to specifically accommodate the effects of stratification. The number $\alpha=0.10$ was adjusted to yield realistic neutral Ekman layers and may still be suspect. The stability functions in Fig. 1 and the critical Richardson number are emerging as remarkably general.

REFERENCES

Businger, J. A., J. C. Wyngaard, Y. Izumi and E. F. Bradley, 1971: Flux-profile relationships in the atmospheric surface layer. *J. Atmos. Sci.*, 28, 181–189.

Caldwell, D. R., C. W. Van Atta and K. N. Helland, 1972: A laboratory study of the turbulent Ekman layer. *Geophys. Fluid Dyn.*, 3, 125–160.

Deardorff, J. W., 1970: A three-dimensional numerical investigation of the idealized planetary boundary layer. *Geophys. Fluid Dyn.*, 1, 377–410.

——, 1973: Note on a paper by D. R. Caldwell, C. W. Van Atta and K. N. Helland. *Geophys. Fluid Dyn.*, 4, 293–296.

Denman, K. L., 1973: A time-dependent model of the upper ocean. *J. Phys. Oceanogr.*, 3, 173–184.

——, and M. Miyake, 1973: Upper layer modification at ocean station 'Papa': Observations and simulation. *J. Phys. Oceanogr.*, 3, 185–196.

Ekman, V. W., 1905: On the influence of the earth's rotation on ocean currents. *Ark. Mat. Astron. Fys.*, 2, No. 11.

Fofonoff, N. P., 1962: Dynamics of ocean currents. *The Sea*, Vol. 1, Wiley.

Gill, A. E., 1969: The turbulent Ekman layer. Dept. Appl. Math. Theoret. Phys., University of Cambridge.

Kato, H., and O. M. Phillips, 1969: On the penetration of a turbulent layer into a stratified fluid. *J. Fluid Mech.*, 37, 643–655.

Kitaigorodsky, S. A., and Yu. Z. Miropolsky, 1970: On the theory of the open-ocean active layer. *Izv. Atmos. Oceanic Phys.*, 6, 97–102.

Kraus, E. B., and J. S. Turner, 1967: A one-dimensional model of the seasonal thermocline. II. The general theory and its consequences. *Tellus*, 19, 98–106.

Kurihara, Y., 1965: On the use of implicit and iterative methods for the time integration of the wave equation. *Mon. Wea. Rev.*, 93, 33–46.

Mellor, G. L., 1973: Analytic prediction of the properties of stratified planetary surface layers. *J. Atmos. Sci.*, 30, 1061–1069.

——, 1975: A comparative study of curved flow and density stratified flow. *J. Atmos. Sci.*, 32, 1287–1282.

——, and J. A. Herring, 1973: A survey of the mean turbulent field closure models. *AIAA Journal*, 11, 590–599.

——, and T. Yamada, 1974: A hierarchy of turbulent closure model for planetary boundary layers. *J. Atmos. Sci.*, 31, 1791–1806.

Minkley, B., 1971: Oceanographic observations at Ocean Station P (50°N, 145°W), Vol. 46, May 15–July 1, 1970. Department of the Environment, Marine Sciences Branch, Pacific Region, Report No. 71-5.

Munk, W. H., and E. R. Anderson, 1948: Notes on a theory of the thermocline. *J. Marine Res.*, 7, 276–295.

Niller, P. P., 1975: Deepening of the wind-mixed layer. Submitted to *J. Fluid Mech.*

Pollard, R. T., P. B. Rhines and R. O. R. Y. Thompson, 1973: The deepening of the wind-mixed layer. *Geophys. Fluid Dyn.*, 3, 381–404.

Richtmyer, R. D., and K. W. Morton, 1967: *Difference Methods for Initial Value Problems*. Interscience, 405 pp.

So, R. M. C., and G. L. Mellor, 1973: Experiments on convex curvature effects in turbulent boundary layers. *J. Fluid Mech.*, 60, 43–63.

Turner, J. S., 1973: *Bouyancy Effects in Fluids*. Cambridge University Press.

——, and E. B. Kraus 1967: A one-dimensional model of the seasonal thermocline. I. A laboratory experiment and its interpretation. *Tellus*, 19, 88–97.

Veronis, George, 1969: On theoretical models of the thermocline circulation. *Deep-Sea Res.*, 16, Suppl., 301–323.

[5] Our own numerical results would conform to this rule if the density and velocity profiles were similar; they are not. However, the $Ri_0^{-\frac{1}{2}}$ behavior is approximately valid. To the extent that this is so, it may be shown that the results are independent of the empirical coefficient α.